Properties of Super-Hydrophobic Copper and Stainless Steel Meshes: Applications in Controllable Water Permeation and Organic Solvents/Water Separation

Sang, Y. C., Albadarin, A. B., Al-Muhtaseb, A. H., Mangwandi, C., McCracken, J. N., Bell, S. E. J., & Walker, G. M. (2015). Properties of Super-Hydrophobic Copper and Stainless Steel Meshes: Applications in Controllable Water Permeation and Organic Solvents/Water Separation. Applied Surface Science, 107-114. DOI: 10.1016/j.apsusc.2015.02.034

Published in:
Applied Surface Science

Document Version:
Peer reviewed version

Properties of Super-Hydrophobic Copper and Stainless Steel Mesh and Their Applications in Controllable Water Permeation and Organic Solvents/Water Separation

Yu Chen Sang[1], Ahmad B. Albadarin[1,2*], Ala'a H. Al-Muhtaseb[3], Chirangano Mangwandi[1], John N. McCracken[1], Steven E.J. Bell[1], Gavin M. Walker[1,2]

[1]School of Chemistry and Chemical Engineering, Queen's University Belfast, Belfast BT9 5AG, Northern Ireland, UK

[2]Department of Chemical and Environmental Sciences, Materials and Surface Science Institute, Synthesis & Solid State Pharmaceuticals Center (SSPC), University of Limerick, Ireland

[3]Petroleum and Chemical Engineering Department, Faculty of Engineering, Sultan Qaboos University, Muscat-Oman.

*Corresponding Author: Dr Ahmad B. Albadarin

Email: Ahmad.B.Albadarin@ul.ie

Department of Chemical and Environmental Sciences, University of Limerick.

Tel: +44 74 6080 5982; fax: +44 28 9097 6524.

ABSTRACT

The wettability and hydrophobicity of super-hydrophobic (SH) meshes is greatly influenced by their topographic structures, chemical composition and coating process. In this study, the properties of copper and stainless steel meshes, coated with super-hydrophobic electrolessly deposited silver were investigated. A new method to test the pressure resistance of super-hydrophobic mesh was applied to avoid any deformation of mesh. Results showed that SH copper mesh and SH stainless steel meshes with the same pore size have almost the same contact angle and the same hydrophobicity. SH copper mesh with a pore size of 122 μm can resist water pressure of 4900 Pa and a decrease of pore size of mesh can increase the pressure resistance of SH copper mesh. The SH copper mesh modified with 0.1M $HS(CH_2)_{10}COOH$ solution in ethanol has a controllable water permeation property by simply adjusting the pH of water solution. SH copper mesh shows super-oleophilicity with organic solvents and so with a water contact angle of 0° and it can be an effective tool for organic solvents/water separation. The separation efficiency of SH copper mesh for separating mixtures of organic solvent and water can be as high as 99.8%.

Keywords: Super-hydrophobic copper mesh; Contact angle; Morphology; Pressure resistance; pH-controllable water permeation; Organic solvents/water separation.

1. INTRODUCTION

The self-cleaning ability of natural super-hydrophobic materials such as lotus leaves and butterfly wings have been simulated by artificial super-hydrophobic surfaces with many potential applications [1]. These surfaces have high water contact angle (θ is higher than 150°), low contact angle (CA) hysteresis [2, 3] and are produced by combinations of lowering the surface free energy and enhancing the surface roughness [1,2]. Moreover, a super-hydrophobic (SH) mesh has unique characteristics: porous surface, mesh-like geometry, great gas permeation performance, high pressure resistance and high striking loading capacity [4-6]. With the development of offshore oil production and maritime traffic, oil–water separation has become a global challenge due to the frequent industrial oily wastewater and oil spill accidents [7-9]. Current studies have reported the excellent performance of SH meshes in the area of controllable water permeation, oil/water separation and water/organic solvents separation. Cao and co-workers [10] developed an oil/water separation mesh with high separation efficiency and intrusion pressure of water. Cao et al have demonstrated that meshes with both super-hydrophobic and oleophobic properties, with a water contact angle higher than 150° and oil contact angle around 140°, can be used to separate oil from water with separation efficiencies reaching 99.3% [10]. Also, La and co-workers have reported a super-hydrophobic and super-oleophilic copper meshes prepared via a simple electrochemical route that were stable over a wide pH range of 2 to 14 and over long periods of time. Results exhibited a potential use of the hybrid copper mesh as a filtering layer for oil and water separation [11]. However, there are some problems which seriously hinder the application of superhydrophobic materials for example poor chemical and mechanical stability, low flexibility of metal meshes, use of complicated procedures and expensive materials [12]. The wettability and hydrophobicity of SH mesh is greatly influenced by their topographic structures [13] and chemical composition [14, 15] including coating process, the size of mesh pores and the thickness of mesh wires [16].

Therefore, the aim of this work was to study the properties of copper mesh and stainless steel mesh coated with super-hydrophobic material. Properties such as contact angle, surface topographic structure, pH-controllable permeation property and organic solvents/water separation capability were examined. A new method to test the pressure resistance of super-hydrophobic mesh was applied to avoid any deformation of mesh. The connection between contact angle and mesh size was also experimentally and mathematically analyzed.

2. MATERIALS AND METHODS

2.1. Materials

Copper meshes (#50 – #120) and stainless steel meshes (#50 – #250) were purchased from The Mesh Company Ltd, UK. Phenolphthalein powders, analytical grades of NaOH and HCl, sodium chloride (NaCl) and silver nitrate (AgNO3); ACS reagents ≥99.0%, were obtained from Sigma Aldrich. Chloroform (≥99%, Sigma Aldrich), n-hexane (95%, Sigma Aldrich) and cyclohexane (99.5%, Sigma Aldrich) were used to make organic solvent/water mixtures. All chemicals were used as received without further purification.

2.2 Preparation of super-hydrophobic copper and stainless steel mesh

Super-hydrophobic copper meshes and super-hydrophobic stainless steel meshes were prepared. Copper meshes were washed with 0.5% HNO_3 (70%, J.T.Baker) and deionised water. The meshes were shaken in 0.02 M $AgNO_3$ (70 cm^3, AnalaR, BDH Chemicals Ltd.) for several min. The meshes were rinsed with deionised water and dried at 70°C. The meshes were then immersed in 100 cm3 of a 0.1 M 1-decanethiol (96%, Alfa Aesar) solution (DT) in ethanol (Absolute ACS grade, J.T.Baker). The mixture was shaken intermittently and left overnight. The obtained meshes were rinsed with absolute ethanol and dried at 70°C [17]. Other surface modifiers used in this experiment were 0.02 M 10-heptadecafluoro-1- decanethiol (HDFT) (96%, Sigma-Aldrich) solution in ethanol (Absolute ACS grade, J.T.Baker) and 0.1 M 11-

mercaptoundecanoic acid, $HS(CH_2)_{10}COOH$, (95%, Sigma-Aldrich) solution in ethanol to achieve different surface properties. Super-hydrophobic stainless steel meshes could not be coated directly since silver could not be deposited on stainless steel materials. Stainless steel meshes must be copper plated first and then coated with silver and modified following the method above. The anode and cathode in this electro-deposition cell were both connected to a rectifier, which was an external supply of direct current. The anode was connected to a copper plate (the positive terminal), and the cathode was connected to the stainless steel mesh that needed to be coated (the negative terminal). 1.5–5 V were applied across the cell. The copper-plating bath was a copper sulfate solution (1.0 mol/L) with some sulfuric acid (a few drops).

2.3.Tests and characterization

2.3.1. Contact angle measurement

The contact angles on the prepared super-hydrophobic copper mesh surfaces with water droplets were monitored using a FTA1000B goniometer instrument (First Ten Angstroms, Ltd). For each sample, five different readings were recorded and the contact angle values were averages of the five measurements made on different points of the sample surface. The FTA 1000B goniometer was composed with a drop dispenser with a syringe and needle, a camera, a stage-sample holder and a backlight. It used proprietary FTA32 software to control the height of the drop dispenser and the volume of the water drop and thus determine the contact angle.

2.3.2. Pressure Resistance Test

A simple and efficient homemade device was designed to test the pressure resistant performance of SH copper mesh (Scheme 1).

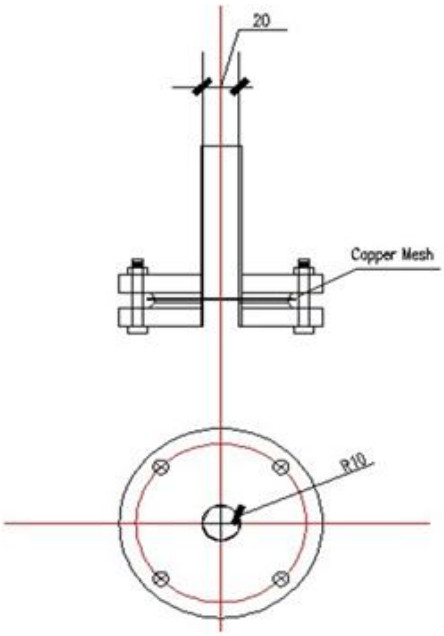

Scheme 1: Device for pressure resistance test.

The SH copper mesh was held between two iron plates, both of which had a hole of 20 mm diameter in the middle. An iron tube was welded to one of the iron plates and a plastic tube with a length of 100 cm was connected with this tube. In order to prevent water leakage from the side of the mesh, asbestos washers with holes of 20 mm diameter in the middle were put between the iron plates as well. The tested mesh was put between the asbestos. The two iron plates were fixed using four bolts tightly. During the test, water was added though the plastic tube into the hole to touch the mesh until the mesh could not resist the high water pressure and water started to leak through mesh pores. The height of water was recorded and the pressure could be calculated. The advantage of this device that it could measure the pressure resistance of mesh accurately without any deformation of mesh surface and without removing the SH coating.

2.3.3. Surface observation

A digital microscope was used to measure the pore size and wire diameter of SH copper mesh.

The topographical microstructure and morphology of the super-hydrophobic copper meshes before and after coating were studied by scanning electron microscopy (Quanta 250 FEG, FEI).

2.3.4. Organic solvent/water separation

10 g deionized water was mixed with 10 g organic solvent (chloroform, n-Hexane and cyclohexane separately). A 20 g mixture of organic solvent and water was used to be separated. The densities of pure water, chloroform, n-hexane and cyclohexane were recorded in advance. After separation, the densities of the liquid in two beakers were measured and the percentage of organic solvent and water in each beaker can be calculated. Further to qualitatively measure the separation efficiency, a mixture of 20 mL of the organic solvent and 30 mL of 0.1 M NaCl aqueous solution was poured slowly onto the SH copper mesh held over a beaker containing 20 mL of 0.1 M $AgNO_3$ aqueous solution [1].

3. RESULTS AND DISCUSSION

3.1. Wettability of super-hydrophobic meshes

Contact angles were measured to study the hydrophobic properties of the coated SH copper mesh and SH stainless steel mesh surfaces. The contact angles were measured with a 10 μL water droplet at ambient temperature (n = 5). Normally contact angles are measured on planar substrates but in this case the droplets were sufficiently large compared to the dimensions of the mesh that the meshes could be treated as being effectively planar for these purposes, as shown in Figure 1.

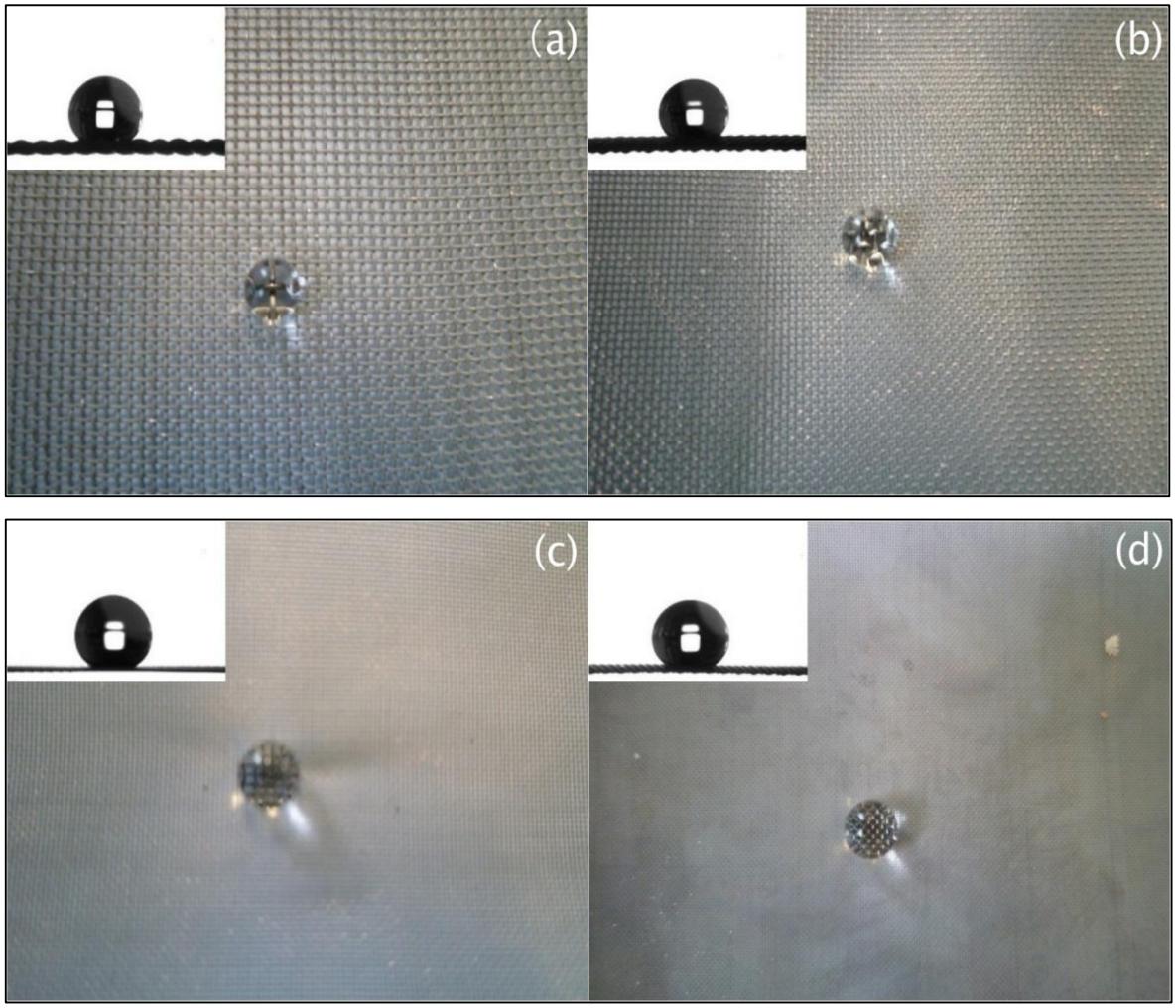

Figure 1: Tilt-view photographs and optical images of water droplets on the HDFT modified copper mesh surface: **(a)** #50 copper mesh; **(b)** #60 copper mesh; **(c)** #100 copper mesh; **(d)** #120 copper mesh.

It can be seen from Table 1, which brings together the data for the SH copper mesh and SH stainless steel mesh with the same pore size, that both metals have almost the same contact angle and showed the same hydrophobicity for equal mesh sizes. This suggests that adding the electro-deposition process does not change the wettability of the coated mesh [18].

Table 1: Contact angle of SH copper meshes with four different sizes.

Samples	**Contact angle (°)**			
	#50	**#60**	**#100**	**#120**

SH copper mesh	137.21	138.82	140.96	141.64
SH stainless steel mesh	137.32	139.21	140.38	142.55

At the same time, meshes with smaller pore size have higher contact angles. The connection between pore sizes of SH meshes and the apparent contact angle has been analyzed mathematically. [2] According to the reformed macroscopic Cassie-Baxter model, the apparent contact angle of SH copper mesh can be given as [2]:

$$\cos\theta_r^{CB} = \frac{b + R(\pi - \theta_e)}{b + R + 0.5d}\cos\theta_e + \frac{b + R\sin(\pi - \theta_e)}{b + R + 0.5d} - 1 \quad (1)$$

where θ_e is the equilibrium contact angle on a smooth surface, and parameters b, R and d are defined in Figure 2.

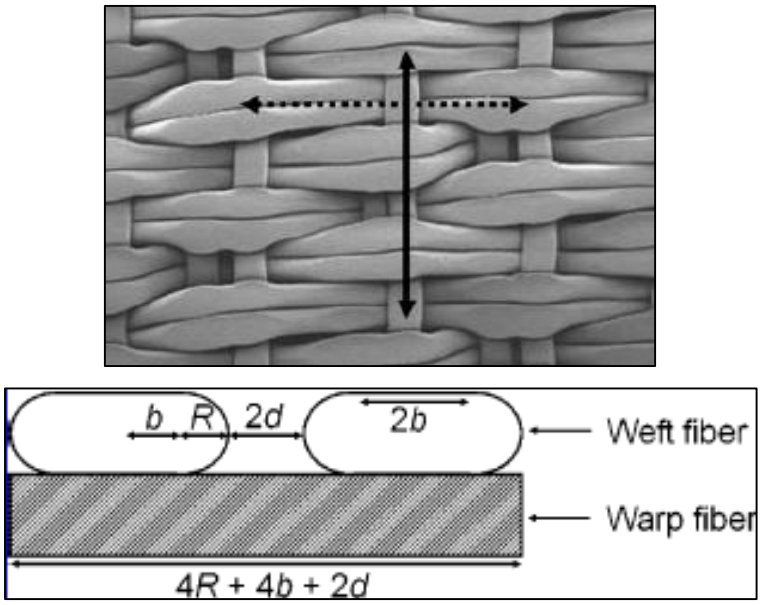

Figure 2: Cross-section view of a calendared woven fabric when it is cut in the warp direction.

The contact angle of smooth copper film surface θ_e was measured to be 51.0° and the contact angle of smooth stainless steel film surface was measured to be 51.1°. The parameters of R and d were determined and are presented in Table 2 and Table 3. Since the mesh wires are

178 columned, the parameter b is equal to 0. The total area of solid-liquid interface f_1 and the total

179 area of liquid-air interface f_2 were calculated using Eqs. (2) and (3) [19]:

180 $$f_1 = r_f f = \frac{4b + 4R\alpha}{4b + 4R + 2d} \quad (2)$$

181 $$f_2 = 1 - f = 1 - \frac{4b + 4R\sin\alpha}{4b + 4R + 2d} \quad (3)$$

182

183 **Table 2:** Sizes of copper meshes.

	Mesh count (per linear inch)	Wire diameter (mm)	Aperture (mm)	Open area
#50	50 wires or holes	0.16	0.348	47%
#60	60 wires or holes	0.16	0.263	39%
#100	100 wires or holes	0.03	0.224	78%
#120	120 wires or holes	0.09	0.122	33%

184 **Table 3:** Sizes of stainless steel meshes.

	Mesh count (per linear inch)	Wire diameter (mm)	Aperture (mm)	Open area
#50	50 wires or holes	0.20	0.308	36.8%
#60	60 wires or holes	0.16	0.263	38.7%
#70	70 wires or holes	0.16	0.203	31.3%
#100	100 wires or holes	0.112	0.142	31.3%
#100A	100 wires or holes	0.056	0.142	-
#120	120 wires or holes	0.09	0.122	33.0%
#250	250 wires or holes	0.04	0.062	37.0%

185 The predicted results of contact angles of SH copper meshes and SH stainless steel meshes are

186 shown in Tables 4 and 5. Clearly, $f_1 + f_2 > 1$ on these rough surfaces, which means that the SH
187 meshes were at Cassie-Baxter state [20].

188 **Table 4:** Comparison of predicted and measured contact angles of SH copper meshes.

Samples	#50	#60	#100	#120
f_1	0.709	0.851	0.266	0.955
f_2	0.789	0.747	0.921	0.716
Contact angle measured (Deg)	137.2	138.8	141.0	141.6
Contact angle predicted (Deg)	139.8	134.8	157.0	131.2

189

190 **Table 5:** Comparison of predicted and measured contact angles of SH stainless steel meshes.

Mesh size (μm)	f_1	f_2	Contact angle measured (Deg)	Contact angle predicted (Deg)
#50	0.885	0.708	137.3	138.7
#60	0.851	0.720	139.2	139.7
#70	0.991	0.673	140.3	135.5
#100	0.992	0.673	140.4	135.4
#100A	0.636	0.790	143.6	146.4
#120	0.955	0.685	142.6	136.6
#250	0.882	0.709	149.9	138.8

191 The predicted values of apparent contact angles of SH meshes are close to the experimental
192 values of apparent contact angles, however, the equilibrium contact angle on a smooth surface
193 plays an important role in the predicted values and a difference of even 0.1° may cause an
194 important error in this final apparent contact angle of around 10°. Thus, the predicted values
195 may be different from the experimental values. This method was first used to predict the
196 apparent contact angle of HDFT modified SH copper mesh and SH stainless steel mesh. The
197 predicted values of contact angle are not only associated with the pore size of mesh, but also

connected with the diameter of wire [21]. The SH meshes with smaller pore size and thinner wire have higher contact angles according to Tables 4 and 5. As can be seen in Table 6, the only difference between SH mesh #100 and SH mesh #100A is the wire diameter.

Table 6: The effect of wire diameter on contact angle of SH stainless steel meshes.

Sample	Pore size (µm)	Wire diameter (µm)	Contact angle measured (Deg)	Contact angle predicted (Deg)
#100	142	112	140.4	135.4
#100A	142	56	143.6	146.4

The diameter of #100A is only half of that of #100. The measured contact angle of #100A is 3.36° higher than that of #100 and the predicted contact angle of #100A is 10.93° higher than that of #100.

Morphology of the surface

The morphology microstructures of the copper meshes before and after coating were observed by scanning electron microscopy. The SEM images of these meshes are shown in Figure 3.

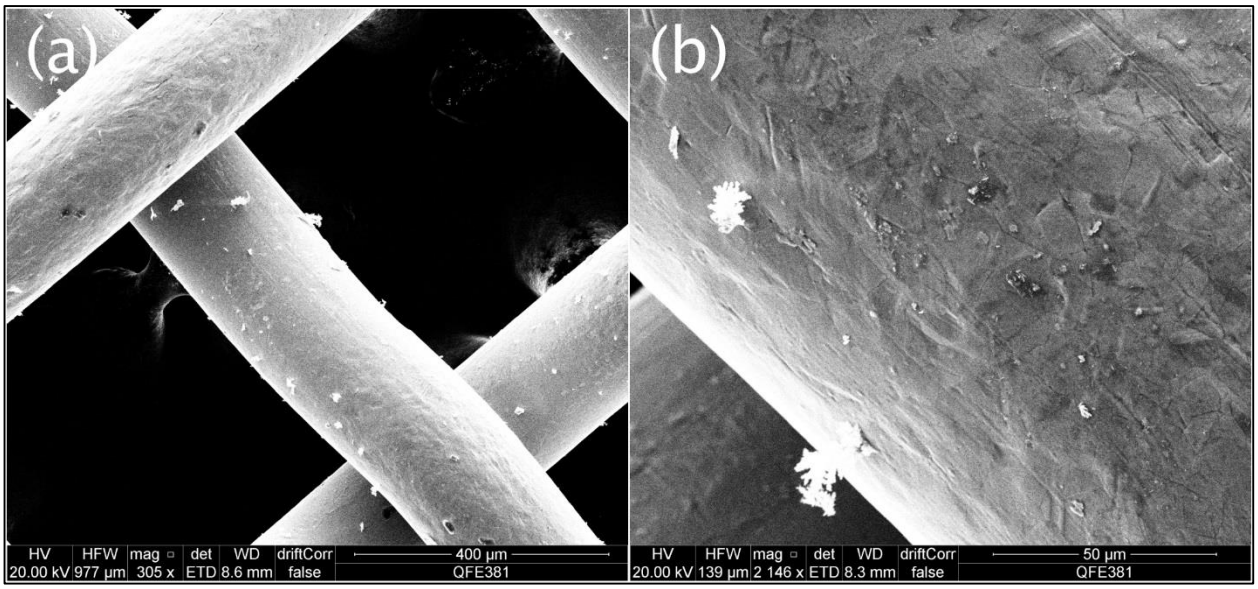

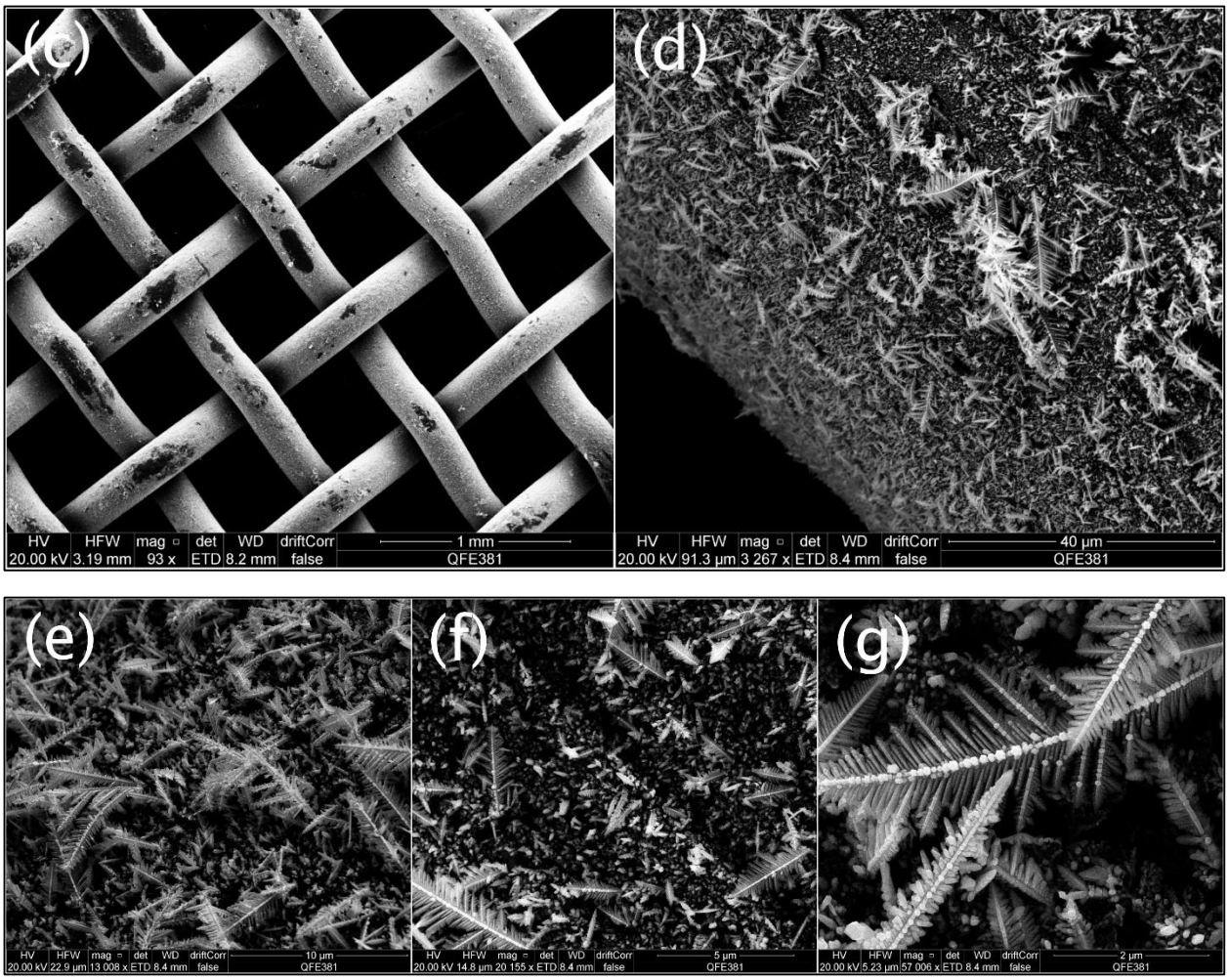

Figure 3: SEM micrographs of copper mesh: **(a) (b)** uncoated mesh; **(c) (d)** coated mesh; **(e) (f) (g)** silver on copper film.

The SEM images indicate that the original copper mesh has a smooth surface with pores of rectangular shape and the mesh wires crisscross together, while the silver forms a thin film in the therstitial opening of the mesh and forms a rough surface with plenty of "leaves" growing on the surface. These "leaves" grow much leafier if the mesh was immersed in silver solution longer, i.e. around 15 min. The "leaves" have a length of around 2–5 μm and they cover all over the mesh wires. Compared with the mesh width of 160 μm, the coated mesh become thicker by around 4–6 μm in width after coated, which can be ignored compared with the width of copper pores. The stainless steel mesh needs to be deposited with copper first before coating.

221 Figure 4 shows an optical image of the #250 stainless steel mesh with a pore size of 122 μm.
222 It has a shiny, smooth metallic surface.

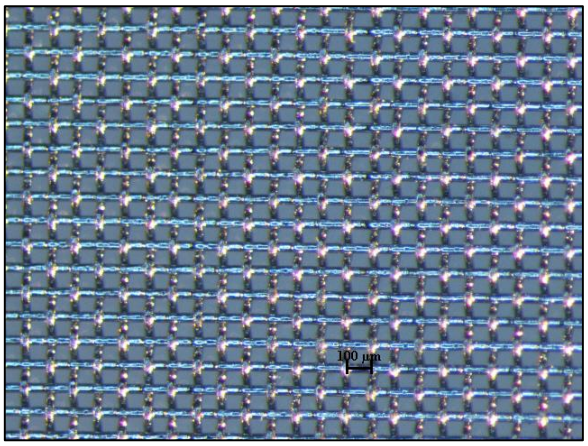

223

224 **Figure 4:** Uncoated #250 Stainless steel mesh.

225 Figure 5 shows stainless steel mesh deposited with copper by electro-deposition and a
226 copper/silver coated SH stainless steel mesh modified with HDFT.

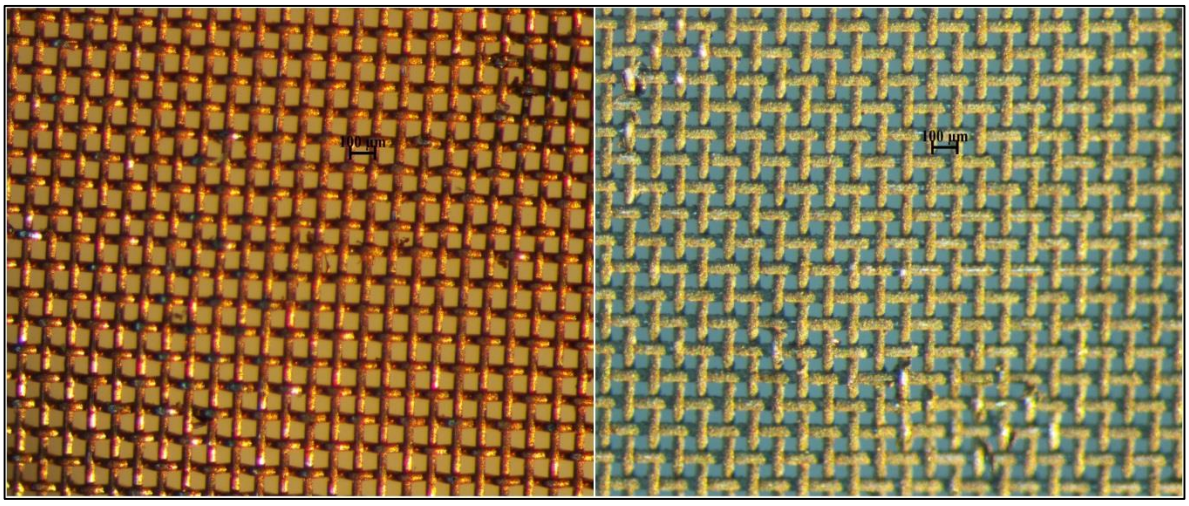

227

228 **Figure 5:** #250 Stainless steel mesh electro-deposited with copper (left); #250 SH stainless
229 steel mesh deposited with copper and silver and modified with HDFT (right).

230 These microscopy images indicate that copper can be evenly deposited on stainless steel
231 surfaces simply through electro-deposition method even on the cross-section part, while the

color turns to be dark yellow after being coated. However, the pores would not be blocked after treatment.

3.2. Pressure resistance evaluation

Pressure resistance property is another important characteristic of hydrophobic porous surface. The height of the water column was recorded and the pressure resistance of the mesh could be calculated as:

$$P = \rho gh \quad (4)$$

where ρ is the water density, g is the gravitational constant and h is the water height. It can be seen from Table 7 that with a decrease of pore size of SH stainless steel mesh, the pressure resistance of SH mesh increases and for #250 SH stainless steel mesh with a pore size of 122 μm, the pressure as high as 4900 Pa can be achieved, which is 50 cm water height.

Table 7: Experimental value of pressure resistance of SH copper mesh.

Sample	**#50**	**#60**	**#100**	**#120**	**#250**
Water height (mm)	37.6	41.0	92	220	500
Pressure resistance (Pa)	368.5	401.8	901.6	2156	4900

At the same time, the copper mesh can be considered as a combination of capillaries [22]. The water level that the SH mesh can resist can be calculated as:

$$H = -\frac{2\gamma \cos\theta^{CB}}{\rho g R} \quad (5)$$

where γ is the surface tension of water, θ is the contact angle of SH copper mesh, and R is the radius of the holes in the mesh wire. The surface tension of water is 71.4 mN/m. The predicted heights of water that the SH meshes can resist are shown in Table 8.

Table 8: Predicted value of pressure resistance of SH copper meshes.

Sample	#50	#60	#100	#120	#250
Predicted Height (mm)	89.42	101.5	142.4	123.8	437.6
Predicted Pressure resistance (Pa)	876.3	994.4	1395.6	1213.7	4288.8

Compared with Table 7, the predicted values in Table 8 are much closer to the measured value when the pore size of mesh is small. With high-pressure resistance of 4900 Pa and tough surface structure, #250 SH stainless steel mesh can be produced as microphones and earphones with strong waterproof property for special uses, such as by firefighters, police officers and divers.

3.3. pH - controllable water permeation

It has been determined that the SH copper mesh has a controllable water permeation property by adjusting the pH of water solution. For acidic water solutions or neutral water, the SH copper mesh is super-hydrophobic, and the water cannot permeate the film because of the large negative capillary effect resulting from the nanostructures. However, for basic solutions with a pH value higher than 8, the film shows super-hydrophilic property, and the solution can permeate the film and keep dropping down as is shown in Figure 6.

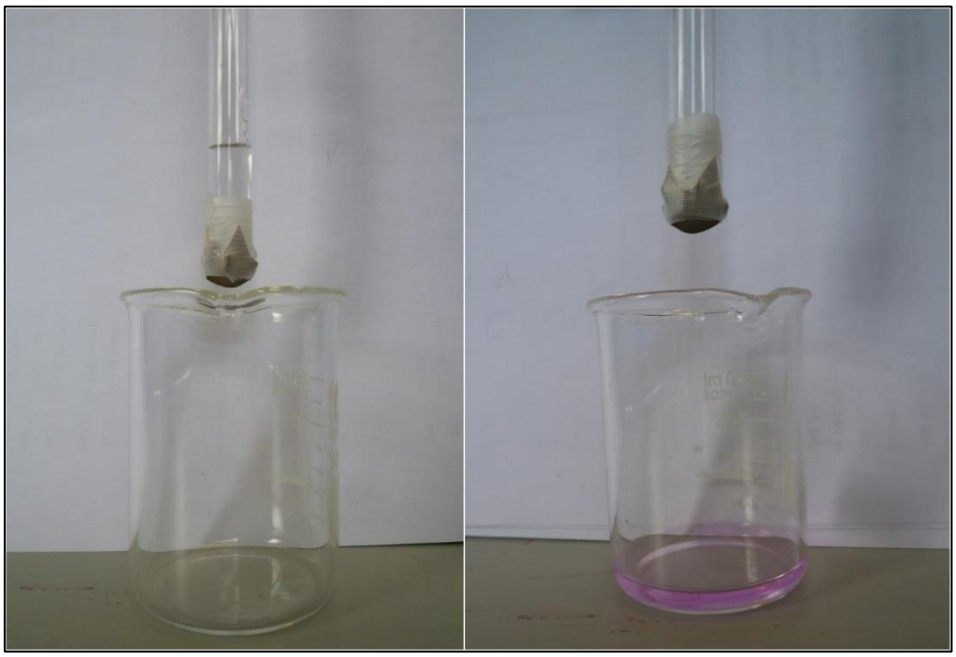

Figure 6: The pH-controllable water permeation device. Neutral water cannot penetrate the rough mesh film (left). Basic water can penetrate the rough mesh film (right). Phenolphthalein was used as pH indicator.

The SH copper mesh was modified with 0.1 M $HS(CH_2)_{10}COOH$ solution in ethanol. It was known that basic solution would react with –COOH structure and led to the de-protonation of thiol chain, while neutral water did not cause any impact on thiol chain. The contact angle of neutral water on SH copper mesh (#100) is higher than 140.96°, while the contact angle of basic water (pH = 14) on SH copper mesh (#100) is as low as 10.24°. By changing the pH of water solution, the controllable permeation of SH copper mesh can be realized simply.

3.4. Separating water and organic solvents

The SH copper mesh used in this study was modified with HDFT. Interestingly, as shown in Figure 7, when a water droplet is laid on SH copper mesh, the mesh shows high super-hydrophobicity and water droplet rolls as a water ball.

278 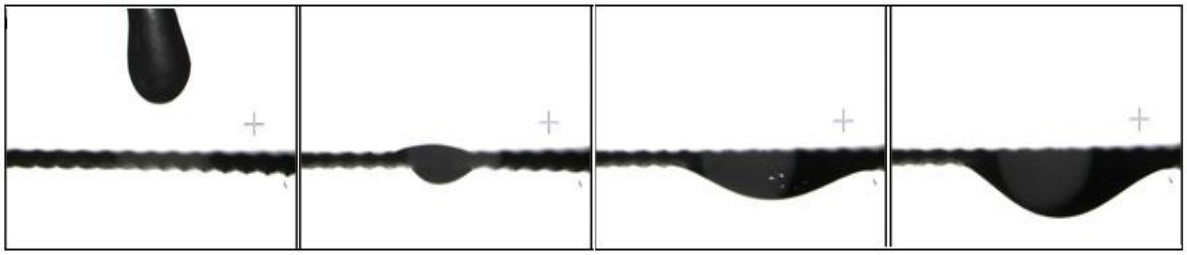

279 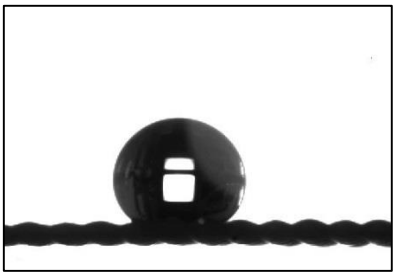

280 **Figure 7:** Organic solvent droplet (Chloroform) on #100 SH copper mesh (top); Water droplet
281 on #100 SH copper mesh (bottom).

282 While organic solvents like chloroform permeate through the mesh freely and drop down
283 easily. The SH copper mesh showed strong super-oleophilicity in this process. The contact
284 angle for chloroform on SH copper mesh (#100) is only 0°. This phenomenon indicates that
285 the SH copper mesh can behave differently for different materials and it can be made an
286 effective tool for organic solvents/water separation. A homemade device was used to separate
287 the mixture of organic solvents and water. A slightly tilted SH copper mesh was placed above
288 two beakers. The mixture of organic solvent and water was dropped through a burette on the
289 mesh at a rate of one droplet per second. During this process, organic solvent droplets would
290 permeate though mesh and fall into the beaker beneath it, while water droplets would roll along
291 the mesh and drop into another beaker. Thus, the mixture (10 g deionized water was mixed
292 with 10 g organic solvent (chloroform, n-Hexane and cyclohexane separately)) was separated.
293 The separation efficiency in Table 9 is the percentage of water that can be recycled from the
294 mixture.

295 **Table 9:** Separation efficiency for different organic solvent/water mixtures.

Mesh size	Efficiency		
	Chloroform	**n-Hexane**	**Cyclohexane**
#50 copper mesh	99.7%	99.8%	99.9%
#60 copper mesh	94.8%	99.0%	98.5%
#100 copper mesh	94.1%	98.8%	93.8%
#120 copper mesh	91.6%	97.7%	92.0%

It can be seen in Table 9 that an efficiency of as high as 99.9% can be achieved using SH #50 copper mesh for cyclohexane and water mixture. While for all the mixtures, a decreasing of the pore size of SH copper mesh causes the decreasing of separation efficiency.

A more sensitive method of detecting water ingress was to set up an experiment such that water penetration would cause a visible precipitate of AgCl. It was experimentally determined that a white precipitate of AgCl could be seen in a 20 mL aqueous solution of 0.1M $AgNO_3$ if as little as 50 μL of 0.005 M NaCl was added. Experiments were then carried out with the #50 copper mesh using a mixture of the organic solvent and aqueous 0.1M NaCl solution. After the separation, the $AgNO_3$ aqueous solution stayed clear, confirming the extremely high organic solvent/water separation efficiency which can be calculated as $\leq 0.01\%$ of the aqueous layer penetrating the film. No decrease in performance was observed after ten cycles of organic solvent/water separation for all mesh sizes (using both density calculations and the $AgNO_3$/NaCl test).

However, SH copper mesh can only separate organic solvents that are not miscible with water. For organic solvents that are miscible with water e.g. ethanol solution, the effect of adding solvent is to decrease the surface tension of the liquid (Table 10). This in turn will reduce the contact angles and also lead ultimately to the liquid penetrating the mesh. The contact angles of the mixtures of ethanol and water with ethanol concentrations from 0% to 100% were

measured (Table 10). Also shown are the compositions where the liquid penetrated the mesh.

Table 10: Contact angle of mixtures of ethanol and water with ethanol concentrations from 0% to 100%.

Concentration%	**Surface tension** [23]	**Contact angle (Deg)**			
	(mN/m) at 298K	**#50**	**#60**	**#100**	**#120**
0	72.01	137.2	138.8	141.0	141.6
10	47.53	121.7	127.2	132.8	127.9
20	37.97	117.9	126.7	131.2	126.6
30	32.98	108.6	123.7	127.8	119.8
40	30.16	110.7	114.2	116.8	111.2
50	27.96	106.0	112.8	111.9	107.4
60	26.23	97.7	102.2	108.4	106.9
70	25.01	97.1	96.2	109.3	96.5
80	23.82	0	94.4	99.7	89.4
90	22.72	0	0	98.5	87.8
100	21.82	0	0	0	0

It is clear that for any given mesh altering the contact angle to values close to or below 90° allows the liquid to penetrate. The composition at which this occurs is different for different meshes, with SH #100 and SH#120 copper mesh able to support mixture with lower surface tensions than the SH #50 and SH#60 meshes.

4. CONCLUSIONS

The properties of copper mesh and stainless steel mesh coated with super-hydrophobic material were investigated including contact angle, surface topographic structure, pH-controllable permeation and its application in organic solvents/water separation. A new method to test the pressure resistance of super-hydrophobic mesh was applied in this study to avoid any deformation of mesh and water leakage from the edges. Based on the results obtained the following conclusions can be drawn:

1. SH copper mesh and SH stainless steel mesh with the same pore size had almost the same contact angle and showed the same hydrophobicity and meshes with smaller pore size have higher contact angles.
2. SH copper mesh with a pore size of 122 μm can resist water pressure of 4900 Pa and a decrease of pore size of mesh can increase the pressure resistance of SH copper mesh. The water level can be mathematically calculated using a capillary combination equation.
3. The SH copper mesh modified with 0.1M $HS(CH_2)_{10}COOH$ solution in ethanol has a controllable water permeation property by simply adjusting the pH of water solution.
4. SH copper mesh shows super-oleophilicity with organic solvents with a contact angle of 0° and it can be made an effective tool for organic solvents/water separation. The separation efficiency of SH copper mesh to separate the mixture of organic solvent and water can be as high as 99.8%.

5. REFERENCES

[1] L. Wu, J. Zhang, B. Li, A. Wang, Mechanical- and oil-durable superhydrophobic polyester materials for selective oil absorption and oil/water separation, Journal of Colloid and Interface Science, 413 (2014) 112-117.
[2] Z.X. Jiang, L. Geng, Y.D. Huang, S.A. Guan, W. Dong, Z.Y. Ma, The model of rough wetting for hydrophobic steel meshes that mimic Asparagus setaceus leaf, Journal of Colloid and Interface Science, 354 (2011) 866-872.
[3] X. Zhu, Z. Zhang, B. Ge, X. Men, X. Zhou, Q. Xue, A versatile approach to produce superhydrophobic materials used for oil–water separation, Journal of Colloid and Interface Science, 432 (2014) 105-108.
[4] T. An, Fabrication of a superhydrophobic water-repellent mesh for underwater sensors, Journal of Sensor Science and Technology, 22 (2013) 100-104.
[5] A.B.D. Cassie, S. Baxter, Wettability of porous surfaces, Transactions of the Faraday Society, 40 (1944) 546-551.
[6] A.M.J. Davis, E. Lauga, The friction of a mesh-like super-hydrophobic surface, Physics of Fluids, 21 (2009) 1-8.

[7] T. Dalton, D. Jin, Extent and frequency of vessel oil spills in US marine protected areas, Marine Pollution Bulletin, 60 (2010) 1939-1945.
[8] Jikang Yuan, Xiaogang Liu, Ozge Akbulut, Junqing Hu, Steven L. Suib, Jing Kong, F. Stellacci, Superwetting nanowire membranes for selective absorption, Nature Nanotechnology, 3 (2008) 332 - 336.
[9] D. Zang, F. Liu, M. Zhang, X. Niu, Z. Gao, C. Wang, Superhydrophobic coating on fiberglass cloth for selective removal of oil from water, Chemical Engineering Journal, 262 (2015) 210-216.
[10] Y. Cao, Z. Zhang, L. Tao, K. Li, Z. Xue, L. Feng, Y. Wei, Mussel-inspired chemistry and Michael addition reaction for efficient oil/water separation, ACS Applied Materials and Interfaces, 5 (2013) 4438-4442.
[11] D.-D. La, T.A. Nguyen, S. Lee, J.W. Kim, Y.S. Kim, A stable superhydrophobic and superoleophilic Cu mesh based on copper hydroxide nanoneedle arrays, Applied Surface Science, 257 (2011) 5705-5710.
[12] L. Wu, J. Zhang, B. Li, A. Wang, Magnetically driven super durable superhydrophobic polyester materials for oil/water separation, Polymer Chemistry, 5 (2014) 2382-2390.
[13] W. Song, F. Xia, Y. Bai, F. Liu, T. Sun, L. Jiang, Controllable Water Permeation on a Poly(N-isopropylacrylamide)-Modified Nanostructured Copper Mesh Film†, Langmuir, 23 (2006) 327-331.
[14] M. Callies, D. Quéré, On water repellency, Soft Matter, 1 (2005) 55-61.
[15] J. Drelich, E. Chibowski, D.D. Meng, K. Terpilowski, Hydrophilic and superhydrophilic surfaces and materials, Soft Matter, 7 (2011) 9804-9828.
[16] A.B. Gurav, Q. Xu, S.S. Latthe, R.S. Vhatkar, S. Liu, H. Yoon, S.S. Yoon, Superhydrophobic coatings prepared from methyl-modified silica particles using simple dip-coating method, Ceramics International, 41 (2015) 3017-3023.
[17] i) I.A. Larmour, G.C. Saunders, S.E.J. Bell, Remarkably Simple Fabrication of Superhydrophobic Surfaces Using Electroless Galvanic Deposition, Angewandte Chemie International Edition, 46 (2007) 1710-1712.
ii) I.A. Larmour, G.C. Saunders, S.E.J. Bell, Compressed Metal Powders that Remain Superhydrophobic after Abrasion, ACS Applied Materials & Interfaces, 2 (2010) 2703-2706.
[18] Weifeng Zhang, Yingze Cao, Na Liu, Yuning Chen, L. Feng, A novel solution-controlled hydrogel coated mesh for oil/water separation based on monolayer electrostatic self-assembly, RSC Advances 4 (2014) 51404-51410.
[19]A. Marmur, Wetting on Hydrophobic Rough Surfaces: To Be Heterogeneous or Not To Be?, Langmuir, 19 (2003) 8343-8348.
[20] A. Siddaramanna, N. Saleema, D.K. Sarkar, A versatile cost-effective and one step process to engineer ZnO superhydrophobic surfaces on Al substrate, Applied Surface Science, 311 (2014) 182-188.
[21] Sanjay Subhash Latthe, Annaso Basavraj Gurav, Chavan Shridhar Maruti, R.S. Vhatkar, Recent Progress in Preparation of Superhydrophobic Surfaces: A Review, Journal of Surface Engineered Materials and Advanced Technology, 2 (2012) 76-94.
[22] Z.X. Jiang, L. Geng, Y.D. Huang, Design and Fabrication of Hydrophobic Copper Mesh with Striking Loading Capacity and Pressure Resistance, The Journal of Physical Chemistry C, 114 (2010) 9370-9378.
[23] G Vhquez, E Alvarez, JM Navaza, Surface Tension of Alcohol + Water from 20 to 50°C, Journal of Chemical and Engineering Data, 40 (1995), 611-614.